

See discussions, stats, and author profiles for this publication at: <https://www.researchgate.net/publication/264431341>

Structure and dynamics of water in crowded environments slows down peptide conformational changes

ARTICLE *in* THE JOURNAL OF CHEMICAL PHYSICS · JULY 2014

Impact Factor: 2.95 · DOI: 10.1063/1.4891465 · Source: PubMed

CITATION

1

READS

37

3 AUTHORS, INCLUDING:



Diego Prada-Gracia

Icahn School of Medicine at Mount Sinai

20 PUBLICATIONS 162 CITATIONS

SEE PROFILE



Francesco Rao

University of Freiburg

42 PUBLICATIONS 1,401 CITATIONS

SEE PROFILE

Structure and dynamics of water in crowded environments slows down peptide conformational changes

Cheng Lu, Diego Prada-Gracia, and Francesco Rao

Citation: *The Journal of Chemical Physics* **141**, 045101 (2014); doi: 10.1063/1.4891465

View online: <http://dx.doi.org/10.1063/1.4891465>

View Table of Contents: <http://scitation.aip.org/content/aip/journal/jcp/141/4?ver=pdfcov>

Published by the [AIP Publishing](#)

Articles you may be interested in

[All-atom molecular dynamics calculation study of entire poliovirus empty capsids in solution](#)

J. Chem. Phys. **141**, 165101 (2014); 10.1063/1.4897557

[Water plays an important role in osmolyte-induced hairpin structure change: A molecular dynamics simulation study](#)

J. Chem. Phys. **137**, 145101 (2012); 10.1063/1.4757419

[Influence of non-universal effects on dynamical scaling in driven polymer translocation](#)

J. Chem. Phys. **137**, 085101 (2012); 10.1063/1.4742188

[Effects of osmolytes on the helical conformation of model peptide: Molecular dynamics simulation](#)

J. Chem. Phys. **134**, 035104 (2011); 10.1063/1.3530072

[Low molecular weight oligomers of amyloid peptides display \$\beta\$ -barrel conformations: A replica exchange molecular dynamics study in explicit solvent](#)

J. Chem. Phys. **132**, 165103 (2010); 10.1063/1.3385470



Launching in 2016!
The future of applied photonics research is here

AIP | APL
Photonics

Structure and dynamics of water in crowded environments slows down peptide conformational changes

Cheng Lu, Diego Prada-Gracia, and Francesco Rao^{a)}

Freiburg Institute for Advanced Studies, School of Soft Matter Research, Albertstrasse 19, 79104 Freiburg im Breisgau, Germany

(Received 26 March 2014; accepted 16 July 2014; published online 30 July 2014)

The concentration of macromolecules inside the cell is high with respect to conventional *in vitro* experiments or simulations. In an effort to characterize the effects of crowding on the thermodynamics and kinetics of disordered peptides, molecular dynamics simulations were run at different concentrations by varying the number of identical weakly interacting peptides inside the simulation box. We found that the presence of crowding does not influence very much the overall thermodynamics. On the other hand, peptide conformational dynamics was found to be strongly affected, resulting in a dramatic slowing down at larger concentrations. The observation of long lived water bridges between peptides at higher concentrations points to a nontrivial role of the solvent in the altered peptide kinetics. Our results reinforce the idea for an active role of water in molecular crowding, an effect that is expected to be relevant for problems influenced by large solvent exposure areas like in intrinsically disordered proteins. © 2014 AIP Publishing LLC. [<http://dx.doi.org/10.1063/1.4891465>]

I. INTRODUCTION

Cell interior is a crowded place.^{1,2} Depending on cell type and growth phase, protein concentrations range between 200 and 300 g/l, whereas that of RNA are in the range of 75–150 g/l, with total concentrations of around 300–400 g/l in organisms like *E. coli*.³ Interestingly, extracellular environments as well are crowded, where other molecules like polysaccharides contribute to keep concentrations very high. As a matter of fact, macromolecular crowding is ubiquitous in living systems.

Notwithstanding, much of the present knowledge both from theory and experiments is about the behavior of macromolecules in highly diluted systems. It has been predicted for quite some time that large effects on the behavior of biomolecules in crowded environments have to be expected.⁴ More recently, experimental works provided evidences for reduced self-diffusion⁵ and enhanced hydrogen exchange rates.⁶ In crowded environments, the available volume is restricted, leading to excluded volume effects. Consequently, compact protein conformations are expected to be favored. The picture however is more complex. For example, protein native states, which are compact, were found to be destabilized in crowded environments.^{6,7} This is apparently due to a competition between stabilizing excluded-volume effects and destabilizing non-specific interactions, including electrostatics. These observations were also confirmed by molecular dynamics studies of chymotrypsin-inhibitor-2 in the presence of either lysozyme or bovine serum albumin crowder molecules.⁸ Finally, it has been found that an optimal concentration exists where the folding rate is the fastest.⁹

Beyond excluded volume effects, the solvent is expected to be a big player for the mediation of the molecular interactions as it has been already observed in aggregation¹⁰ and protein-protein binding.¹¹ In highly crowded environments, the fraction of interfacial water was found to be around 30%–70% of the total water in the cell,¹² meaning a separation between macromolecules of around 1–2 nm.¹³ In these conditions, water structure and dynamics are probably more similar to confined water¹⁴ than the bulk solvent. This is expected to impact several properties of water, including a smaller dielectric constant,^{11,15–17} a decreased hydrogen-bond coordination,¹⁸ a slowing down of the dynamics,¹⁹ and a retarded hydrogen bonds exchange.^{20,21}

In this work, we present an extensive molecular dynamics simulation study with the aim to further elucidate the relationship between biomolecular conformational changes and water mediation in crowded environments. The disordered peptide (GlySer)₂ was analyzed at different concentrations. Evidence was provided for an active role of the solvent in the slowing down of the peptide conformational dynamics upon crowding. Our results suggest that the modified water structure and dynamics in crowded environments play a nontrivial role for biomolecular conformational changes. This would be especially relevant for those cases where large solvent exposed areas are involved, like for intrinsically disordered proteins and protein-protein recognition.

II. METHODS

A. Molecular dynamics simulations

To mimic biological crowding environments, an interesting class of systems is given by (GlySer)_x peptides. These peptides have been used in experiments for quite some time as flexible linkers.^{22,23} Short stretches of this peptide represent an interesting system for theoretical studies, showing a

^{a)} Author to whom correspondence should be addressed. Electronic mail: francesco.rao@frias.uni-freiburg.de. Telephone: +49 (0)761 203 97336. Fax: +49 (0)761-203 97451.

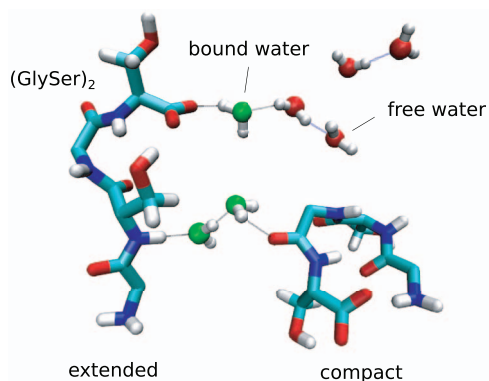


FIG. 1. Schematic representation of two neighbor $(\text{GlySer})_2$ peptides and selected waters inside the simulation box. The extended and compact conformations of the peptide are shown. Two types of water molecules are defined: *bound* water molecules (green, waters directly bonded to one of the peptides); *free* water molecules (red, all the others). A water bridge between two peptides through two (green) water molecules is shown. Gray lines represent hydrogen bonds.

dynamic interchange between compact and extended structures. They are characterized by a complex free-energy surface and, at the same time, can be extensively simulated due to the small number of atoms.^{24,25} In this work, a four residues peptide, $(\text{GlySer})_2$, was considered (Fig. 1). We neutralized ionic N- and C-terminus of $(\text{GlySer})_2$ by *ACE* and *CT3* residues, respectively, to reduce peptide-peptide interactions.

To examine the effect of crowding, we performed a series of fully atomistic molecular dynamics (MD) simulations of highly concentrated solutions. Six molecular setups were built by increasing the number of $(\text{GlySer})_2$ peptides in the box (see Table I), ranging from concentrations between 93.35 g/l and 560.12 g/l. For reference, we also ran a system with only one $(\text{GlySer})_2$ that effectively represents the case of infinite dilution. Initial systems were generated by placing the peptides in random orientations with no overlap by using the program Packmol.^{26,27} All systems were solvated in TIP3P water in a cubic box with periodic boundary conditions.

All simulations were performed using the all-atom CHARMM force-field version 27^{28,29} as implemented in the program ACEMD,³⁰ running on NVIDIA GTX680 graphics cards. Equilibration was obtained by running 10 ns long simulations in the NPT ensemble with pressure of 1 atm and temperature of 300 K. After equilibration, production

runs were extended to 8 μs in the NVT ensemble at 300 K. The Langevin algorithm with a damping factor of 0.1,³¹ an integration time step of 4 fs using mass repartitioning^{30,32} with a saving frequency of 100 ps was used. Pressure was controlled with the Berendsen barostat.³³ The particle mesh Ewald (PME) method was employed for the calculation of electrostatic interactions.³⁴ Interactions were smoothly truncated at a cutoff distance of 9 Å, using a switching function becoming effective at 7.5 Å. Trajectories were analyzed with the program WORDOM,^{35,36} and AQUALAB (raolab.com).

B. Hydrogen bond lifetimes

To investigate water-water hydrogen bond lifetimes, NVT simulations of about 80 ns in length have been continued from the original runs to produce high resolution trajectories with a saving frequency of 0.5 ps. This was necessary due to the short lifetimes of water hydrogen bonds.

The hydrogen-bond definition applied in this manuscript considers the oxygen-oxygen distance (r_{OO}) and the $\angle\text{OOH}$ angle (Θ) between two water molecules.³⁷ Cutoffs of, respectively, 3.5 Å and 30° were used. Peptide-water and peptide-peptide hydrogen bonds were calculated by selecting the donor and acceptor atoms in each peptide and using the same cutoffs of water-water hydrogen bonds.

Hydrogen bond kinetics was also calculated on trajectories generated with a more standard simulation protocol (1 fs integration time and no mass repartitioning), finding exactly the same results.

C. Radius of gyration

The structural differences between the infinite dilution and high crowding cases were investigated by analyzing the radius of gyration (R_g). Given the large flexibility of these peptides, R_g is a good observable for a global structural analysis.^{22–25} The radius of gyration was calculated with the program WORDOM,^{35,36} considering only the CA atoms of the peptide.

D. First passage time distributions

Peptide kinetics was investigated by first-passage-times (*FPT*) analysis.^{24,25,38} This represents the distribution of times to reach a given target conformation from any other snapshot of the trajectory. Arrival times depend on the definition of the target only and not on the detailed decomposition of the trajectory.²⁵

III. RESULTS

A. $(\text{GlySer})_2$ peptides as molecular crowders

In experiments a frequently used molecular crowder is the polyethylene glycol (PEG) molecule.^{39,40} Simulations of the $(\text{GlySer})_2$ peptide in a box with water and a high concentration of PEG molecules would represent an interesting molecular setup to study crowding in a controlled manner. However, being the $(\text{GlySer})_2$ peptide per se both flexible and

TABLE I. Molecular dynamics simulations details.

Box ^a (Å)	N_{peptide} ^b	N_{water} ^c	Concentration (g/l)
39.89	1	2070	9.33
40.04	10	1961	93.35
40.04	20	1813	186.71
40.01	30	1673	280.06
39.93	40	1505	373.42
40.02	50	1375	466.78
40.01	60	1228	560.12

^aSide length of the cubic box after NPT equilibration.

^bNumber of peptides in the box.

^cNumber of water molecules.

weakly interacting, itself would also represent a good candidate to mimic cell crowding.^{22,23} In experiments, to use $(\text{GlySer})_x$ peptides to mimic crowding is less convenient because they undergo a more expensive synthesis process to produce them at any length with respect to PEG molecules. On the other hand, for simulations they would allow a much better sampling when multiple identical copies are used both as probe and crowders.

This is the approach that was taken here: to run simulations of the $(\text{GlySer})_2$ peptide with an increasing number of identical copies, acting as molecular crowders. One of the major advantages of this strategy is that a much increased statistics is obtained from each simulated trajectory because data are collected from all the peptides in the box. Starting with an isolated peptide solvated in water, the concentration was progressively increased by adding multiple peptide copies while keeping the simulation box constant in size (see Sec. II). Following this procedure, six different simulation setups were generated ranging from 10 to up to 60 peptides, reaching concentrations similar to the ones found inside the cell. Details on the actual simulation setups after NPT equilibration are shown in Table I.

Fig. 2(a) presents the number of $(\text{GlySer})_2$ intra-chain and inter-chain hydrogen bonds, respectively, shown in gray and black as a function of the number of peptides in the box. The former is constant while inter-chain interactions tend to increase at higher concentrations. Even in the most crowded case, peptides make in average only 1.4 hydrogen bonds between each other, indicating that $(\text{GlySer})_2$ is weakly

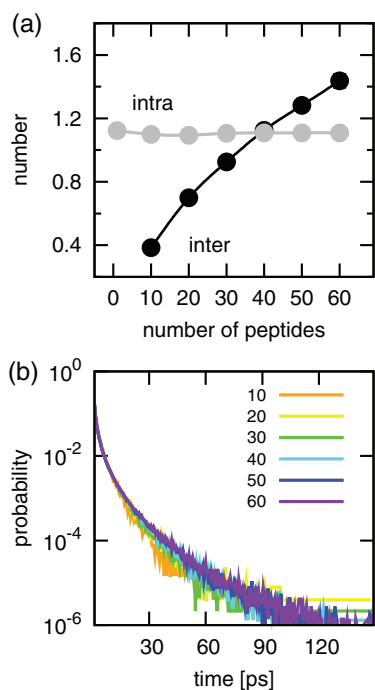


FIG. 2. $(\text{GlySer})_2$ as molecular crowder. (a) Average number of intra-chain and inter-chain hydrogen bonds per peptide as a function of the number of peptides in the simulation box. Standard deviations were found lower than 2.8×10^{-2} and 4.5×10^{-2} for the intra and inter-chain case, respectively. (b) Lifetime distributions of inter-chain (peptide-peptide) hydrogen bonds for each setup. Hydrogen-bond kinetics was calculated from the extended NVT simulations (80 ns, see Sec. II).

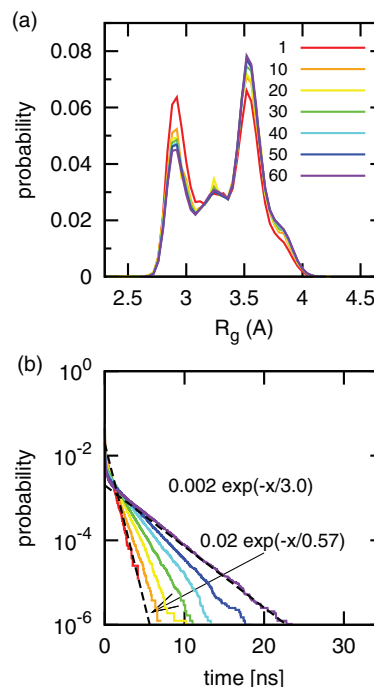


FIG. 3. Thermodynamics and kinetics of $(\text{GlySer})_2$ peptides. (a) Average distribution of the backbone radius of gyration R_g . Distributions were calculated from the entire trajectory (8 μs , see Sec. II) and averaged over all the simulated peptides. Standard deviations for each point were calculated using 10 average distributions corresponding to segments 1/10 of the total trajectory. These errors were omitted for the sake of clarity (the largest deviations found with 10 and 60 peptides were $\sigma = 3.7 \times 10^{-3}$ and 2.4×10^{-3} , both in $R_g = 3.54$ where the difference between these distributions is 8×10^{-3}). (b) Average distribution for the first passage time to the compact conformation (see Sec. II). The latter is defined as peptide snapshots with $R_g \leq 2.90$.

interacting with no signs of aggregation. Moreover, the life-time of such interactions (Fig. 2(b)) is short-lived and independent from concentration, reinforcing the idea that $(\text{GlySer})_2$ peptides represent good molecular crowders.

B. Thermodynamics and kinetics of $(\text{GlySer})_2$ peptides in crowded environments

From a thermodynamic point of view, the peptide conformational space is weakly affected by crowding. This is shown in Fig. 3(a) by the distribution of the radius of gyration R_g . The distribution of the isolated peptide (red) shows two distinct peaks, indicating an equilibrium between compact and extended structures. A similar behavior was also observed for the case with charged terminals.^{24,25} As the concentration was increased, the population of the extended conformation slightly increased from 52.4% to 61.8% for, respectively, the isolated case and the 60 peptide setup (the population is estimated as the integral of the distribution with $R_g \geq 3.3$ Å). Apart from this small difference, the general picture is the same at higher concentrations with a balance between compact and extended conformations, indicating that molecular crowding does not play a big role in the relative free energy of the stable conformations visited by the peptide.

Being a projection, the distribution of the R_g is not very useful for a rigorous analysis of the molecular kinetics.²⁵ To

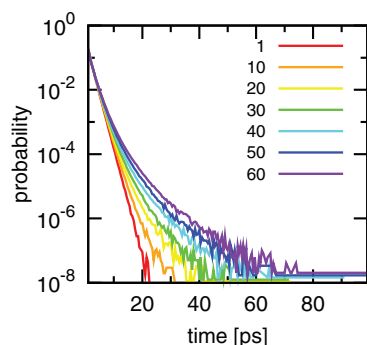


FIG. 4. Water-water hydrogen bonds lifetime distributions. Hydrogen-bond kinetics was calculated from the extended NVT simulations (80 ns, see Sec. II).

improve this, the first passage time (FPT) distribution was calculated (see Sec. II). The FPT represents the distribution of times to go from any snapshot along the MD trajectory to the first occurrence of a target conformation. The latter was defined as peptide compact structures with $R_g \leq 2.9$ Å (first peak of Fig. 3(a)). FPT distributions at different concentrations are shown in Fig. 3(b). According to these data, peptide kinetics is highly influenced by molecular crowding. Although maintaining the same exponential decay $\exp(-t/\tau)$ (linear scaling on a log-linear plot like in the figure), the characteristic time τ goes from 0.57 ns to 3 ns for the diluted and most crowded cases, respectively. As such, despite the thermodynamics is only moderately affected, molecular crowding dramatically slows down peptide conformational dynamics by roughly a factor of five.

C. Water-water hydrogen-bond kinetics in crowded environments

The cause of peptide slowing down does not seem to be due to direct peptide-peptide interactions. In fact, few hydrogen bonds are formed between them (as illustrated before in Fig. 2(a)) as well as the lifetime of these interactions is not affected by the increased concentration (Fig. 2(b)). Surprisingly, this is not the case of water. In Fig. 4 the lifetime distribution of water-water hydrogen bonds is presented.⁴¹ The plot shows that molecular crowding dramatically affects the behavior of the kinetics going from an exponential decay for the diluted system to a pronounced stretched exponential behavior in the case of higher concentrations.

To better understand the mechanism behind this effect, water molecules were labeled in different ways according to their interaction with the peptides. Waters that are directly bonded to the peptide (*bound*, green molecules in Fig. 1) and waters that are not (*free*, red molecules). Analysis of the hydrogen-bond kinetics for the two cases revealed interesting differences. First, as one might have expected, crowding does not affect the hydrogen-bond kinetics between free waters (Fig. 5(a)). Second, hydrogen-bond kinetics between free and bound waters is only marginally affected by molecular crowding (Fig. 5(b)). Third, a pronounced stretched exponential behavior develops for the hydrogen-bond kinetics of bound-bound water molecules (Fig. 5(c); an example of

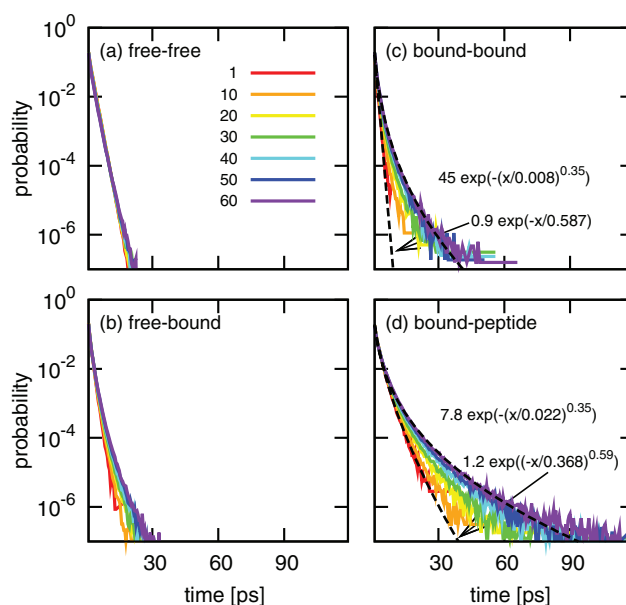


FIG. 5. Water-water hydrogen bonds lifetime distributions for different water configurations: (a) free-free, (b) free-bound, (c) bound-bound, and (d) bound-peptide. See main text for details. Hydrogen-bond kinetics was calculated from the extended NVT simulations (80 ns).

this interaction is shown in Fig. 1 between the two green water molecules). This is a strong response to crowding, going from exponential decay to stretched where the stretching factor becomes smaller and smaller as the concentration increases. For the most crowded case of 60 peptides the stretching factor becomes as low as 0.35 (see also Fig. 5(c) for all fitting parameters). This type of hydrogen bond represents water bridges between peptides (Fig. 1). At high concentrations more than 80% of these waters are bonded to different peptides, effectively creating water bridges composed of two hydrogen bonded water molecules. As a matter of comparison, water-peptide hydrogen bonds were also calculated, showing a similar slowing down (Fig. 5(d)). As observed in Ref. 42 the decay form is again the one of a stretched exponential where the stretching factor goes from 0.59 to 0.35 as the concentration increases.

Summarizing this part, water-water hydrogen bond lifetimes are affected by molecular crowding only in the case when both water molecules are bound to a peptide, effectively forming water bridges between peptides. The decay goes from exponential to stretched exponential, resembling the behavior of peptide-water hydrogen bonds. Altogether these observations suggest that this type of water-water hydrogen bonds behave qualitatively differently between the diluted and crowded cases, representing a possible explanation for the slowing down of the peptide conformational dynamics.

D. Water solvation around peptides

The number of waters around the peptide within 4 Å (close waters) decreases substantially with concentration going in average from 55 to 32 as shown in Fig. 6(a). This behavior reflects the presence of the other peptides in the box. Accordingly, the number of hydrogen bonded waters

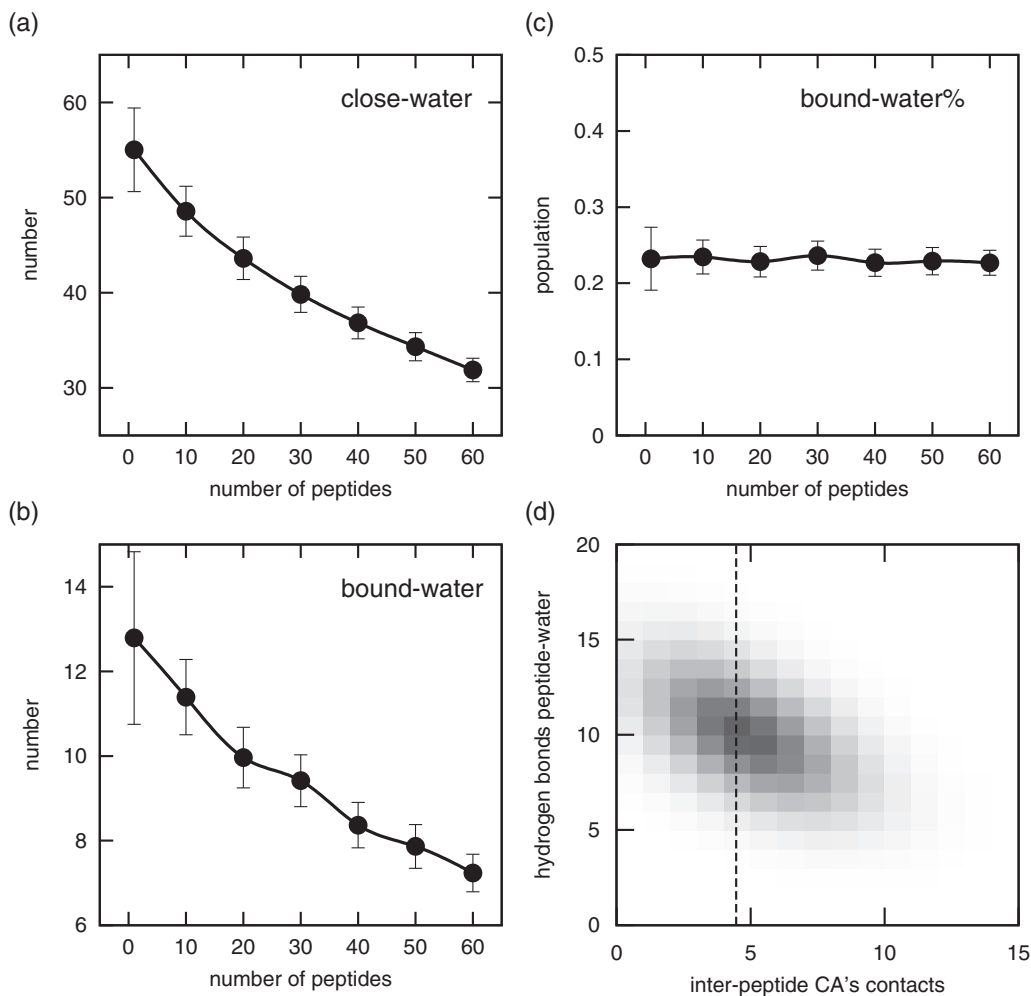


FIG. 6. Water solvation around peptides as a function of concentration. (a) The average number of waters per peptide within 4 Å and standard deviations. (b) The average number of hydrogen bonded waters per peptide and standard deviations. (c) The percentage of bound-water molecules per peptide (i.e., the ratio of the two above quantities) with propagated standard deviations. (d) 2D histogram of the CA-CA inter-peptides contacts (5.5 Å cutoff) and the number of hydrogen bonds with water per peptide for the highest concentration case (60). The average number of CA-CA contacts for random distributions of peptides in vacuum with the same concentration is shown as a dashed vertical line.

decreases as well. Fig. 6(b) shows that this number decreases from 13 to 7 per peptide in average. Instead the fraction of hydrogen bonded waters, i.e., the ratio between the other two former numbers, stays constant (Fig. 6(c)). The number of hydrogen bonds per water molecule tends as well to decrease as the concentration is increased although much more slightly in agreement with recent calculations by other groups.⁴³

These results seem to suggest a progressive dehydration of the peptides as the concentration increases. To check whether there was any significant contribution of aggregation in our simulations, a 2D map was calculated reporting on the correlation of inter-peptides CA-CA contacts and the number of water-peptide hydrogen bonds. Fig. 6(d) shows this map for the highest concentration. Interestingly, the abscissa of the center of the distribution is very close to the average number of contacts a peptide would have if peptides were considered as non-interacting (this was calculated by generating a set of random configurations of the box taking into account only steric clashes). The plot indicates that the larger the number of inter-peptide contacts the lower the bonded waters to the

peptides. However, no sign of aggregation was found (bottom right region of the plot).

IV. DISCUSSION

In this study, extensive molecular dynamics simulations have been performed to investigate the thermodynamics and kinetics of a short disordered peptide in the presence of molecular crowders at different concentrations. Crowding was achieved by increasing the number of identical copies of the peptide keeping the volume approximately constant. According to the present study, molecular crowding does not alter dramatically the thermodynamics of the peptide. On the other hand, the kinetics is affected, showing a slowing down of five folds.

Being the peptides weakly interacting among each other (a requisite to be good crowders), our results provided evidence for a non-trivial role of the solvent for the peptide slowing down. At higher concentrations, peptide hydration is altered both in the number of hydrogen bonded waters and hydrogen bond kinetics. It was found that water molecules in the

interfacial gap between peptides form an adhesive hydrogen-bond network between the interfaces. This arises from long-lived water-water hydrogen bonds with a lifetime strongly dependent on the concentration of the molecular crowders. Interestingly, these bonds not only became long lived but changed their decay form from exponential to stretched exponential: a change that suggests the presence of multiple timescales for the water kinetics in the interfacial gaps.

An interesting way to prove that the peptide slowing down is due to the increased water-water hydrogen bond lifetime would have been to study the same system with an implicit solvent. Although theoretically possible, it is not particularly relevant because the free-energy landscape of $(\text{GlySer})_2$ is not well characterized by any of the implicit solvent we tried.²⁴ This limitation makes this comparison not very useful.

It is worth noting that other studies showed a similar perturbation of water structure and kinetics as we observed. For example, water in hydrophilic pores, like Vycor glass, has a perturbed hydrogen-bonded network with an average coordination number going from 3.6 in the bulk to about 2.2.¹⁸ Moreover, force microscopy experiments suggested that confined water between hydrophilic surfaces that are less than about 2 nm apart exhibits an increased viscosity by several orders of magnitude compared to the bulk solvent.^{44,45} Both observations are in line to what was observed here.

In conclusion, although excluded volume effects can predict many of the aspects of molecular crowding, other physical factors need to be considered to develop a better understanding of the behavior of biomolecules in a cellular environment. Our results reinforce the idea for a non-trivial behavior of the solvent. A phenomenon which can be of great importance in cases where large solvent exposed surfaces play a role like in intrinsically disordered proteins or in protein-protein recognition.

ACKNOWLEDGMENTS

This work was supported by the Excellence Initiative of the German Federal and State Governments.

¹R. J. Ellis and A. P. Minton, *Nature (London)* **425**, 27 (2003).

²A. P. Minton, *J. Biol. Chem.* **276**, 10577 (2001).

³S. B. Zimmerman and S. O. Trach, *J. Mol. Biol.* **222**, 599 (1991).

⁴R. J. Ellis, *Curr. Opin. Struct. Biol.* **11**, 114 (2001).

⁵F. Roosen-Runge, M. Hennig, F. Zhang, R. M. Jacobs, M. Sztucki, H. Schober, T. Seydel, and F. Schreiber, *Proc. Natl. Acad. Sci. U.S.A.* **108**, 11815 (2011).

⁶K. Inomata, A. Ohno, H. Tochio, S. Isogai, T. Tenno, I. Nakase, T. Takeuchi, S. Futaki, Y. Ito, H. Hiroaki *et al.*, *Nature (London)* **458**, 106 (2009).

⁷A. C. Miklos, M. Sarkar, Y. Wang, and G. J. Pielak, *J. Am. Chem. Soc.* **133**, 7116 (2011).

⁸M. Feig and Y. Sugita, *J. Phys. Chem. B* **116**, 599 (2012).

⁹A. Dhar, A. Samiotakis, S. Ebbinghaus, L. Nienhaus, D. Homouz, M. Gruebele, and M. S. Cheung, *Proc. Natl. Acad. Sci. U.S.A.* **107**, 17586 (2010).

¹⁰D. Thirumalai, G. Reddy, and J. E. Straub, *Acc. Chem. Res.* **45**, 83 (2012).

¹¹M. Ahmad, W. Gu, T. Geyer, and V. Helms, *Nat. Commun.* **2**, 261 (2011).

¹²J. Spitzer, *Microbiol. Mol. Biol. Rev.* **75**, 491 (2011).

¹³P. Ball, *Chem. Rev.* **108**, 74 (2008).

¹⁴D. Russo, R. K. Murarka, J. R. Copley, and T. Head-Gordon, *J. Phys. Chem. B* **109**, 12966 (2005).

¹⁵R. Harada, Y. Sugita, and M. Feig, *J. Am. Chem. Soc.* **134**, 4842 (2012).

¹⁶S. Tanizaki, J. Clifford, B. D. Connelly, and M. Feig, *Biophys. J.* **94**, 747 (2008).

¹⁷F. Despa, A. Fernández, R. S. Berry *et al.*, *Phys. Rev. Lett.* **93**, 228104 (2004).

¹⁸H. Thompson, A. K. Soper, M. A. Ricci, F. Bruni, and N. T. Skipper, *J. Phys. Chem. B* **111**, 5610 (2007).

¹⁹G. Stirnemann, F. Sterpone, and D. Laage, *J. Phys. Chem. B* **115**, 3254 (2011).

²⁰A. C. Fogarty, E. Duboué-Dijon, F. Sterpone, J. T. Hynes, and D. Laage, *Chem. Soc. Rev.* **42**, 5672 (2013).

²¹D. Laage, G. Stirnemann, F. Sterpone, R. Rey, and J. T. Hynes, *Ann. Rev. Phys. Chem.* **62**, 395 (2011).

²²O. Bieri, J. Wirz, B. Hellrung, M. Schutkowski, M. Drewello, and T. Kiefhaber, *Proc. Natl. Acad. Sci. U.S.A.* **96**, 9597 (1999).

²³A. Möglich, K. Joder, and T. Kiefhaber, *Proc. Natl. Acad. Sci. U.S.A.* **103**, 12394 (2006).

²⁴F. Rao and M. Spichty, *J. Comput. Chem.* **33**, 475 (2012).

²⁵G. Berezovska, D. Prada-Gracia, S. Mostarda, and F. Rao, *J. Chem. Phys.* **137**, 194101 (2012).

²⁶L. Martínez, R. Andrade, E. G. Birgin, and J. M. Martínez, *J. Comput. Chem.* **30**, 2157 (2009).

²⁷J. M. Martínez and L. Martínez, *J. Comput. Chem.* **24**, 819 (2003).

²⁸B. R. Brooks, R. E. Bruccoleri, B. D. Olafson, S. Swaminathan, M. Karplus *et al.*, *J. Comput. Chem.* **4**, 187 (1983).

²⁹B. R. Brooks, C. L. Brooks, A. D. Mackerell, L. Nilsson, R. J. Petrella, B. Roux, Y. Won, G. Archontis, C. Bartels, S. Boresch *et al.*, *J. Comput. Chem.* **30**, 1545 (2009).

³⁰M. Harvey, G. Giupponi, and G. D. Fabritiis, *J. Chem. Theory Comput.* **5**, 1632 (2009).

³¹G. Bussi, D. Donadio, and M. Parrinello, *J. Chem. Phys.* **126**, 014101 (2007).

³²M. Harvey and G. De Fabritiis, *J. Chem. Theory Comput.* **5**, 2371 (2009).

³³H. J. Berendsen, J. P. M. Postma, W. F. van Gunsteren, A. DiNola, and J. Haak, *J. Chem. Phys.* **81**, 3684 (1984).

³⁴T. Darden, D. York, and L. Pedersen, *J. Chem. Phys.* **98**, 10089 (1993).

³⁵M. Seeber, M. Cecchini, F. Rao, G. Settanni, and A. Caflisch, *Bioinformatics* **23**, 2625 (2007).

³⁶M. Seeber, A. Felling, F. Raimondi, S. Muff, R. Friedman, F. Rao, A. Caflisch, and F. Fanelli, *J. Comput. Chem.* **32**, 1183 (2011).

³⁷A. Luzar D. Chandler *et al.*, *Phys. Rev. Lett.* **76**, 928 (1996).

³⁸F. Rao and M. Karplus, *Proc. Natl. Acad. Sci. U.S.A.* **107**, 9152 (2010).

³⁹A. P. Minton, *Curr. Opin. Biotechnol.* **8**, 65 (1997).

⁴⁰L. A. Munishkina, E. M. Cooper, V. N. Uversky, and A. L. Fink, *J. Mol. Recogn.* **17**, 456 (2004).

⁴¹D. Prada-Gracia, R. Shevchuk, and F. Rao, *J. Chem. Phys.* **139**, 084501 (2013).

⁴²S. Bandyopadhyay, S. Chakraborty, and B. Bagchi, *J. Am. Chem. Soc.* **127**, 16660 (2005).

⁴³J. T. King, E. J. Arthur, C. L. Brooks, and K. J. Kubarych, *J. Am. Chem. Soc.* **136**, 188 (2014).

⁴⁴R. Major, J. Houston, M. McGrath, J. Siepmann, and X.-Y. Zhu, *Phys. Rev. Lett.* **96**, 177803 (2006).

⁴⁵J. Gao, R. Szożkiewicz, U. Landman, E. Riedo *et al.*, *Phys. Rev. B* **75**, 115415 (2007).